Supplementary Information: Graphene Episulfide : Covalent Sulfur Addition to Graphene Surfaces

Experiments

Computational

proposed structure GS_2.

Experiments

For a better understanding and reproducibility of the reaction, an example of dumbbell reaction chamber with reactants is shown in Figure S1. In order to validate the necessity of having both reactants for the synthesis of the product and its location, control measurements were performed. Firstly, the process was done with only sulfur, as seen in Figure S2, the only differences seen between the Raman spectra before and after reaction can be attributed to a quenching when the sample is taken out the ovens and a resulting phase transition of the sulfur. Secondly, the process was done with only HOPG, no modifications of the Raman spectra were observed in the low frequencies near the 520 cm^{-1} peak. Near the G band region, some phenomena are observed, a small and wide D band appears as well as a D' band possibly due to the heat treatment, however no traces of the graphene episulfides peaks. Concerning the 2D band area, the 2D peak decreases and shifts, and again there are no traces of the product. Finally, during the Raman measurements of the process with both sulfur and HOPG, measurements were taken on the surface of the substrate (see Figure S3) before and after the reaction, in this case, no graphene episulfides or contaminants peaks were seen.

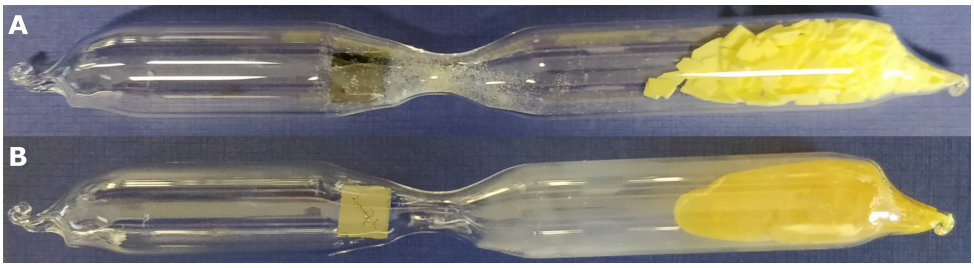

Fig. S1: **Picture of dumbbell shaped chamber before and after reaction. A.** Reaction chamber with freshly cleaved 1 by 1 cm HOPG sample and pristine sulfur before reaction. Thin sulfur powder can be seen near the bottleneck and the HOPG, it is due to the introduction of sulfur pellets in the glass tube however due to the size and geometry of the cleaved sample within the cylindrical part of the chamber no powder was in direct contact with the sample. **B.** Reaction chamber with reacted cleaved HOPG sample and quenched sulfur after reaction. Due to the temperature decrease conditions and the induced chemical vapor transport, one can see that no sulfur is in the graphene compartment and all the sulfur condenses within its compartment.

Control Raman measurements

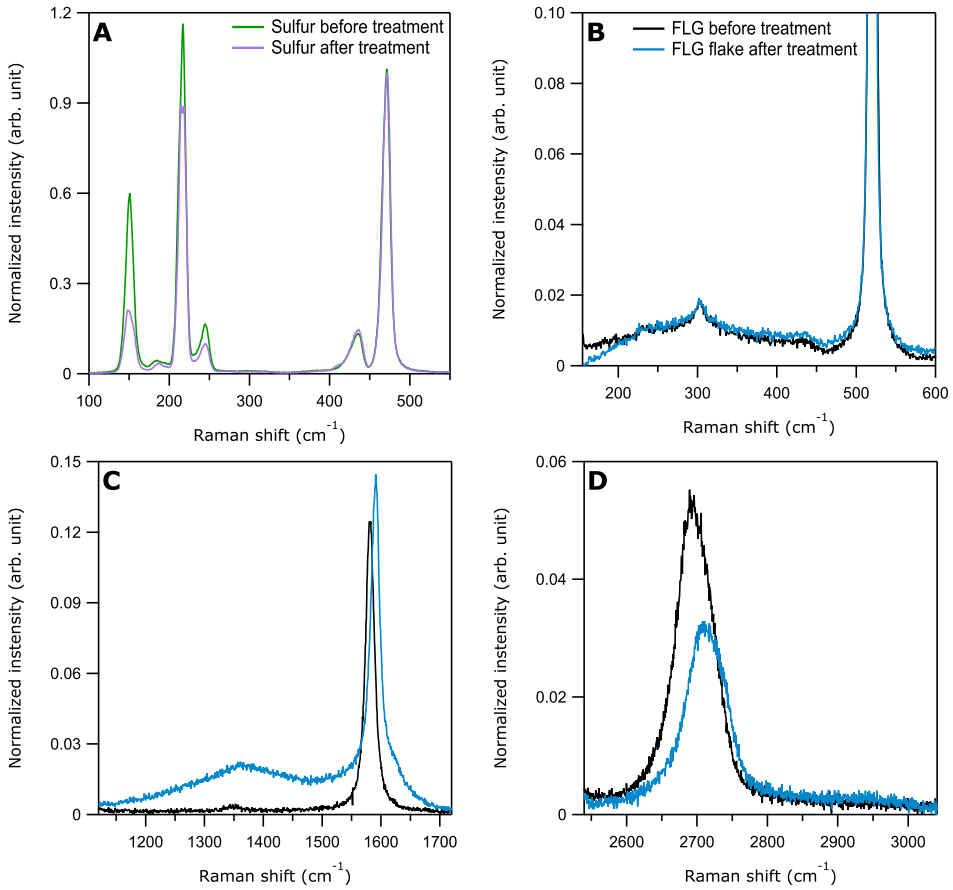

Fig. S2: **Raman control experiments (I). A.** Raman spectra of elemental sulfur before and after treatment without the presence of graphene. **B-D** Raman spectra of a few-layer graphene flake (3 nm-9 layers) before and after treatment without the presence of sulfur reactant in the Si, G and 2D bands regions respectively. Duration and conditions of temperature, pressure and atmosphere composition were kept the same as the synthesis protocol, respectively 24 h, 473 K and 643 K, 0.75 atm of Argon.

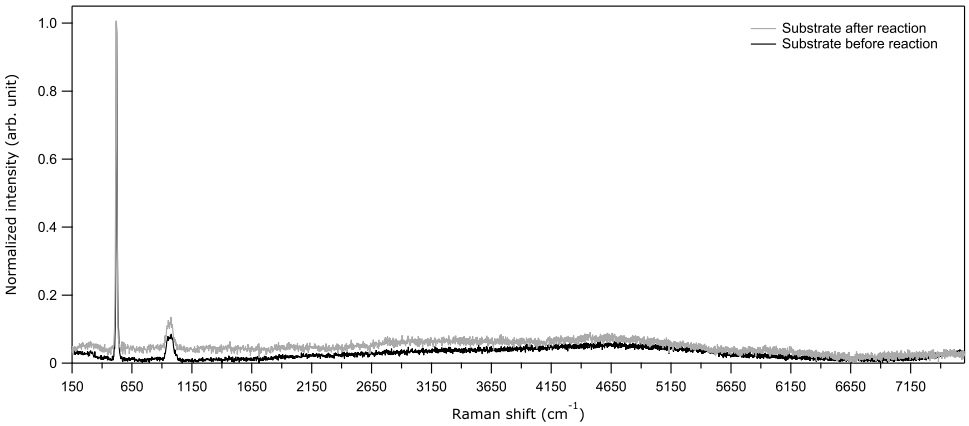

Fig. S3: **Raman control experiments (II).** No peak of graphene episulfide can be detected on the substrate after 24h reaction indicating that sulfur species react only with graphene.

PL - Raman spectroscopy

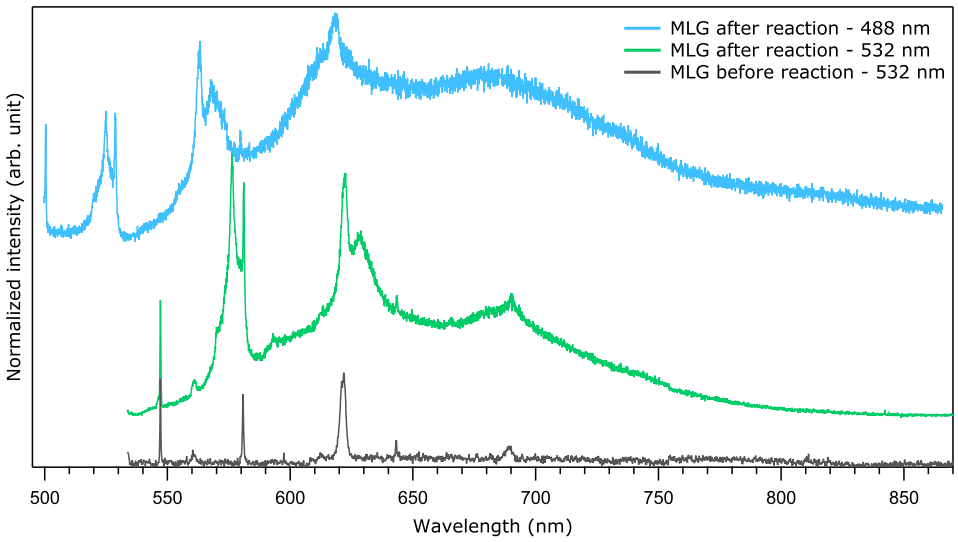

Fig. S4: **Visible luminescence of graphene episulfide under two laser excitation wavelengths.** PL spectra of a pristine few-layer graphene flake (black) and the reacted compound recorded under 488 nm (blue) and 532 nm (green) laser excitation.

Supplementary Raman measurements

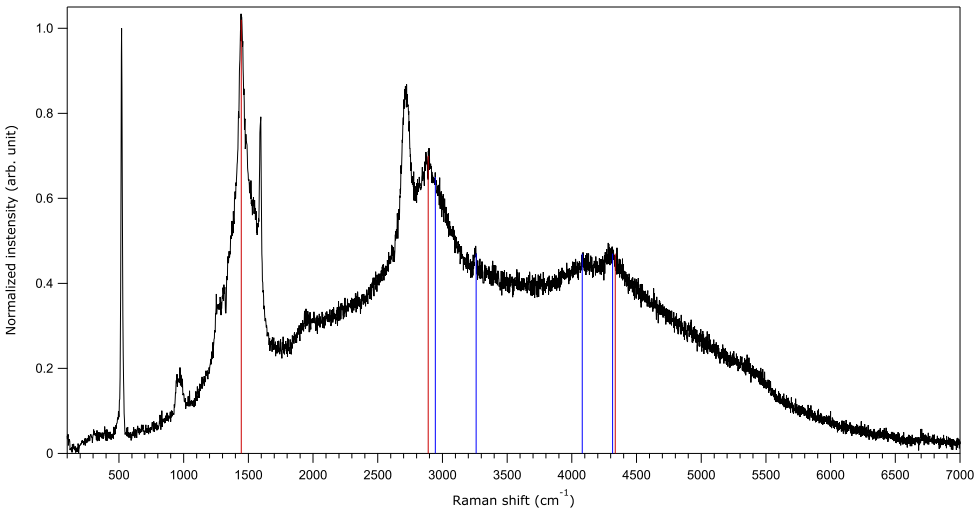

Fig. S5: **Identification of Raman overtones.** In red, the 1445 cm^{-1} peak and the first and second overtones at 2890 and 4335 cm^{-1}. In blue, pristine graphene peaks: D+G, 2D', D+2D and G+2D respectively at 2945, 3260, 4080 and 4315 cm^{-1} [1].

.

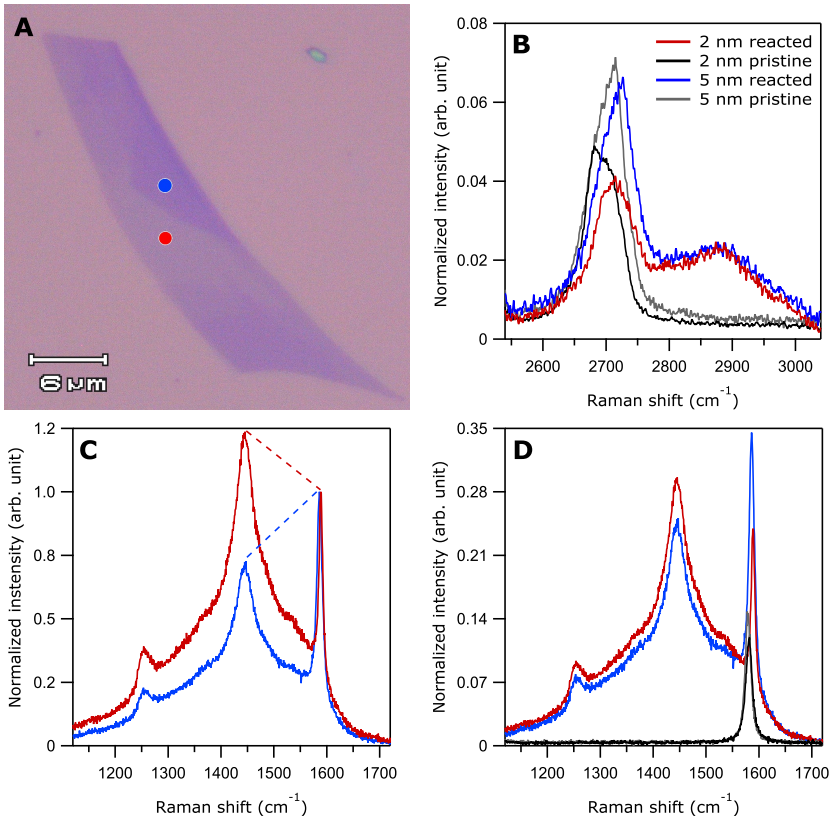

Fig. S6: **Confocal Raman spectra recorded in two distinct regions of the GS flake presented in Figure 1. A.** Optical image of the flake indicating the locations of the selected regions for Raman measurements corresponding to plateaus of 2 nm (red) and 5 nm (blue) in thickness. **B.** Raman spectra in the 2D band region normalized with the integrated Si band intensity (I/I_{Si} ratio) before and after reaction. **C and D.** Raman spectra of selected regions (see panel A) after reaction in the G band region. The spectra are normalized relative to the integrated G band intensity (I/I_G ratio) in panel C and relative to the integrated Si band intensity (I/I_{Si} ratio) before and after reaction in panel D. Note that the spectra taken before and after reaction are in black and red for the 2 nm region and in grey and blue for the 5 nm region, respectively. The shifts before and after reaction are $\Delta G = +8$ cm^{-1} and $\Delta 2D = +15$ cm^{-1} for 2 nm region and $\Delta G = +6$ cm^{-1} and $\Delta 2D = +10$ cm^{-1} for the 5 nm region.

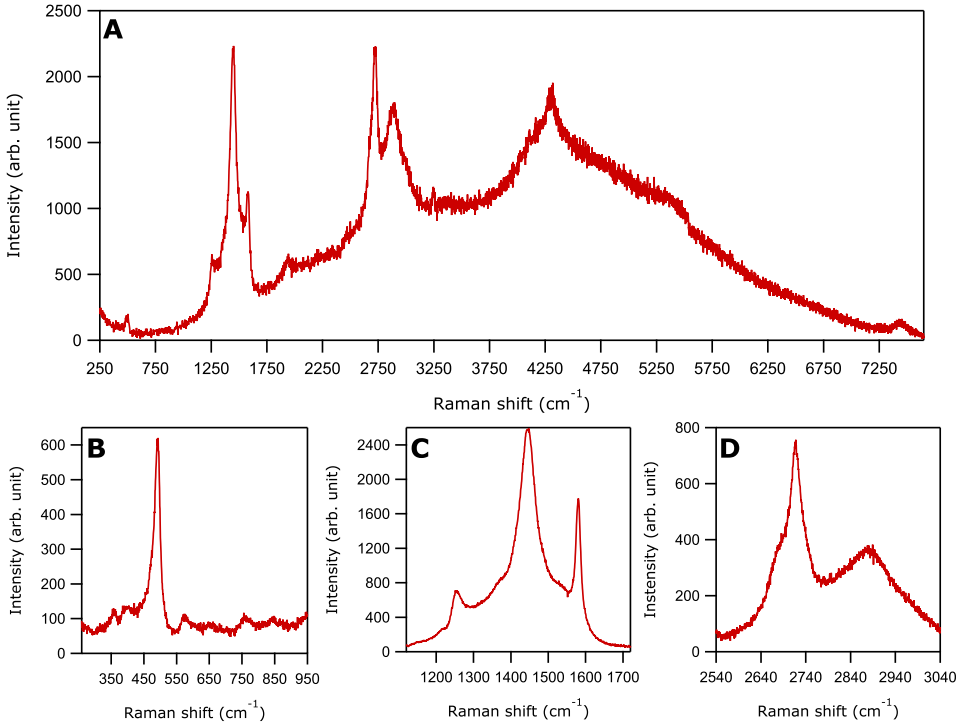

Fig. S7: **Raman spectra of the cleaved HOPG sample after reaction analyzed by XPS. A.** Full Raman spectrum recorded under 532 nm laser excitation. **B-D** Zooms of the Raman spectra taken after reaction in the S-band, G-band and 2D-band regions. The Raman responses are strong despite the large thickness (in microns) due to a longer reaction time (7 days) suggesting a slow diffusion process into the bulk.

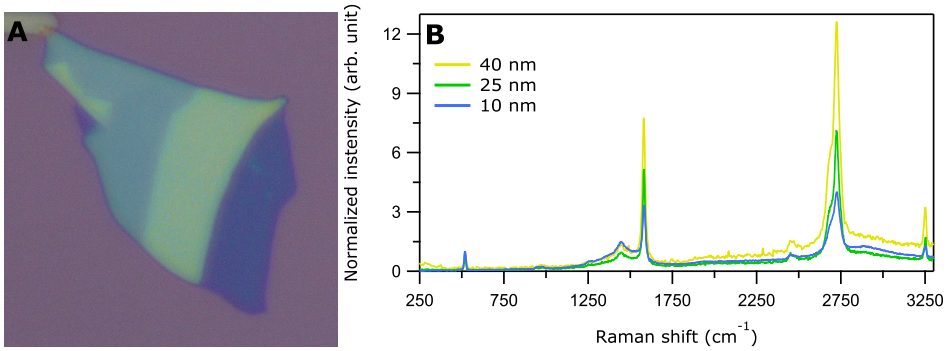

Fig. S8: **Thickness-dependent Raman spectra of GS materials. A.** Optical image (23×23 μm) of a GS flake showing three distinct regions of 10 nm (right), 25 nm (left) and 40 nm (middle) thickness. **B.** Raman spectra measured on the three regions after reaction with sulfur.

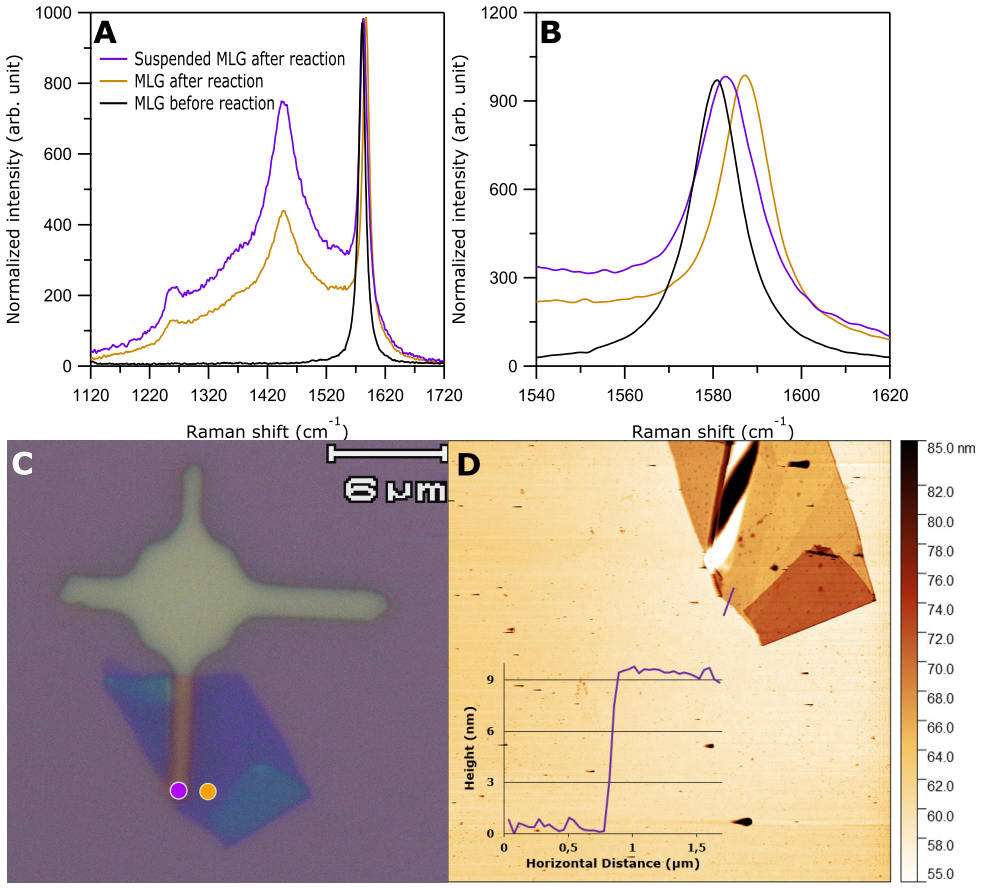

Fig. S9: **Preliminary results obtained on a suspended GS flake. A.** Comparison of the Raman spectra measured before reaction (black) and after reaction on a suspended (purple) and non-suspended (yellow) area of the reacted sample. **B.** Normalized Raman intensities highlighting different values of the G-band shift between the freestanding (purple) and supported (yellow) parts of the GS flake. **C.** Optical image of a partially suspended few-layer graphene flake. **D.** AFM image (20×20 μm) of the FLG flake recorded after the reaction.

Supplementary XPS and UPS results

In order to complete the validation of the necessity of having both reactants for the synthesis of the product, control measurements were performed. In XPS, the process was done with only HOPG, without sulfur, in the same conditions of temperature, pressure and atmosphere composition. As seen in Figure S10, there is no changes between the pristine HOPG and the control HOPG.

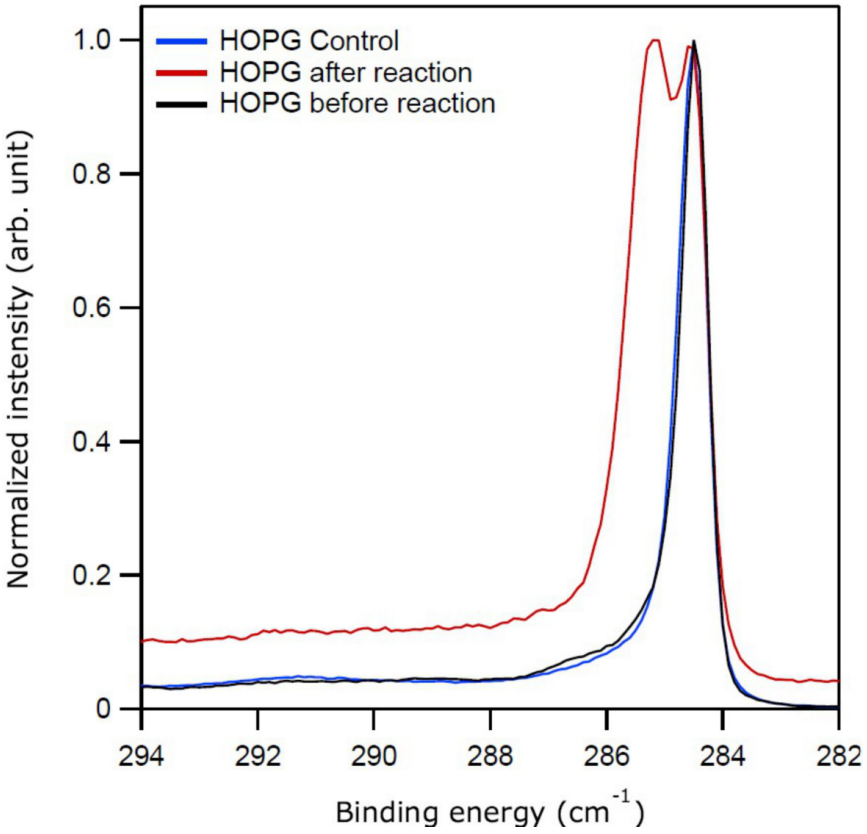

Fig. S10: **Comparison of C 1s XPS spectra of HOPG recorded before and after reaction, and of HOPG under the same treatment without sulfur.** Reaction conditions were kept as described in Methods, only sulfur was removed from the reaction chamber for control. In this Figure, XPS peaks are normalized on the C sp^2 of graphite before reaction for comparison.

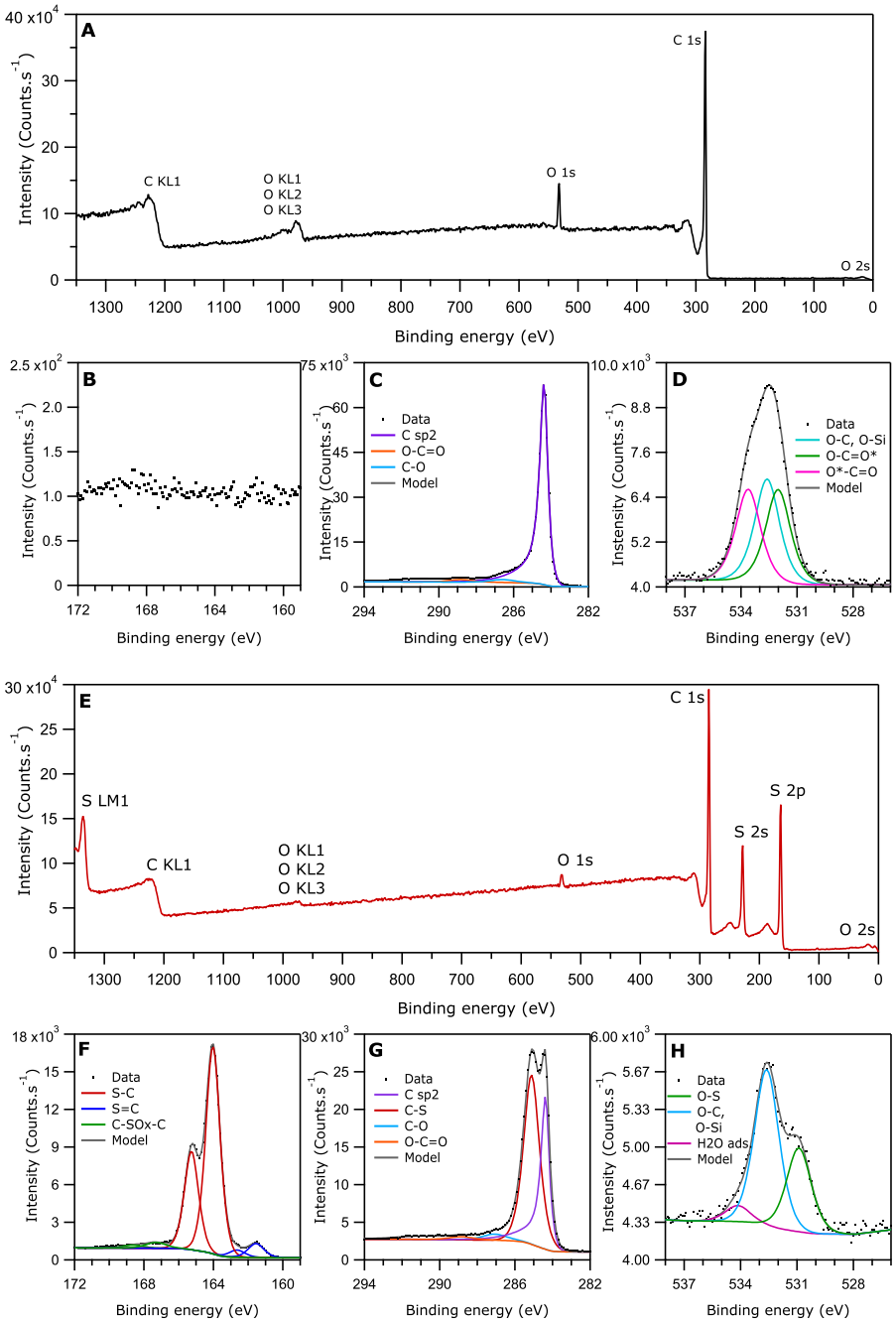

Fig. S11: **Complete XPS measurements of freshly cleaved HOPG sample before and after reaction with sulfur. A.** XPS spectrum survey of cleaved HOPG before reaction. **B-D.** High resolution spectra of the respective S 2p, C 1s and O 1s regions of cleaved HOPG before reaction. **E.** XPS spectrum survey of cleaved HOPG after reaction. **F-H.** High resolution spectra of the respective S 2p, C 1s and O 1s regions of cleaved HOPG after reaction.

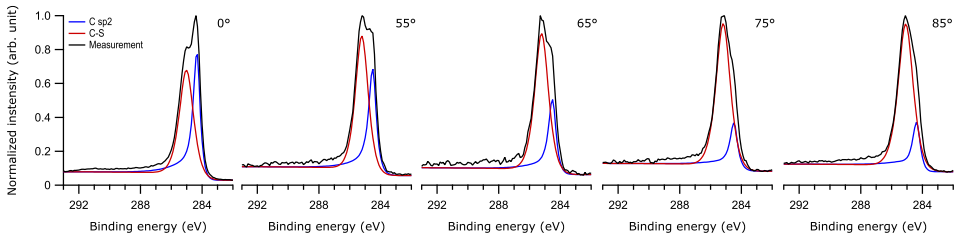

Fig. S12: **Angle-resolved XPS measurements of freshly cleaved HOPG taken after a reaction with sulfur.** Fits to the peaks at 285.5 eV (red) and 284.4 eV (blue) are also shown. The angles are determined from the normal incidence and allow progressively an aimed depth of 8.94 to 0.78 nm.

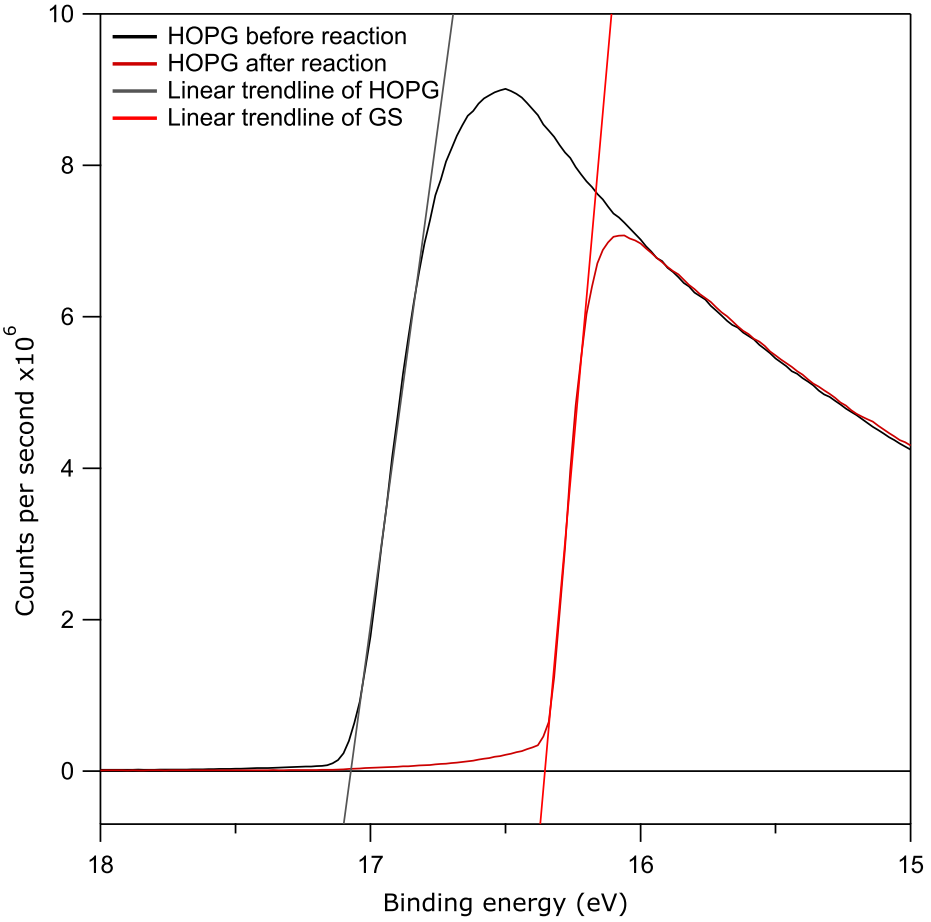

Fig. S13: **Zoom in the UPS spectra of a cleaved HOPG sample taken before and after reaction.** The extraction via line fits of the workfunction change gives a $\Delta\phi = +0.6$ eV.

Atomic Force Microscopy

In order to remove the hypothesis of a possible of a polymeric coating instead of a compound, AFM measurements have been performed. Figure S14 displays a comparison between the pristine and reacted sample for two samples. Changes in the topography and marbles can be observed after reaction. The increase of roughness can be explained by the strain applied by the episulfidation of graphene domains.

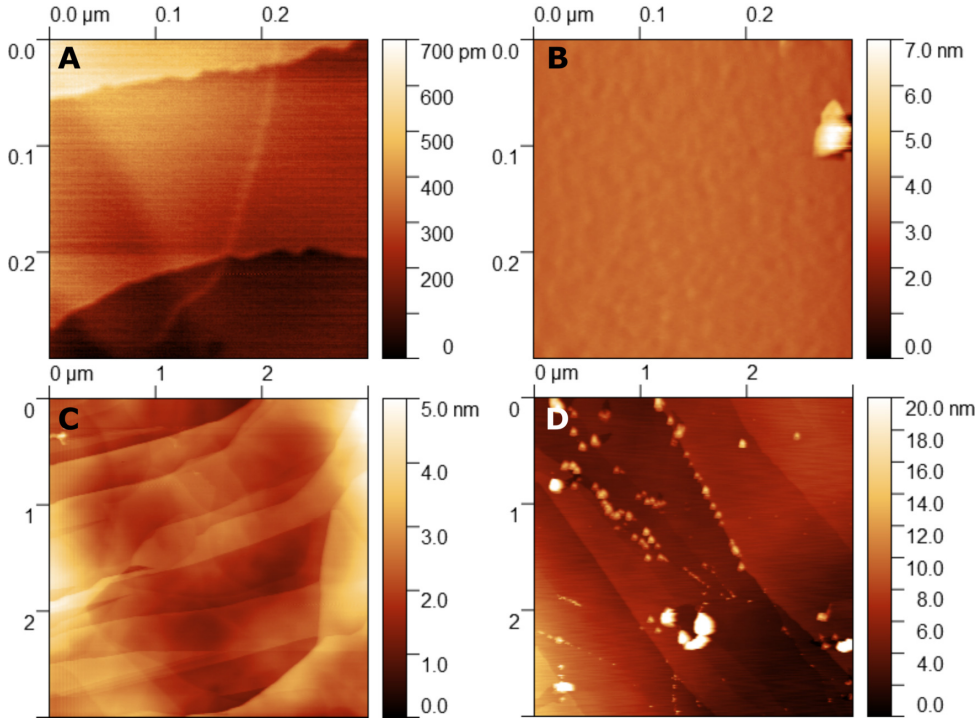

Fig. S14: **AFM study of few microns HOPG before and after reaction. A.** AFM image (300×300 nm) of FLG flakes before reaction; **B.** AFM image (300×300 nm) of HOPG after reaction. **C.** AFM image (3×3μm) of HOPG before reaction. **D.** AFM image (3×3 μm) of HOPG after reaction. The RMS roughness of regions of flat surfaces before (A) and after (B) reaction are 0.27 Å and 1.67 Å, respectively.

Transmission Electron Microscopy

Transmission electron microscopy (TEM) coupled with energy dispersion spectroscopy (EDS) has been performed on graphene nanopellet flakes and the results are presented in Figure S15. The yellow rectangle in panel C marks the region investigated by EDS images of elemental mapping. To verify the homogeneity of the reaction, we analyzed the carbon and the sulfur distributions and the results in panels D-F show that the distribution is uniform throughout the flakes. This is with the Raman results discussed in the main text. The carbon distribution (green) also shows a good colocalization between the sulfur (in red) and the carbon distribution. The colocalization image in panel F was obtained using COL Finder plugin of IMAGE J software and show that up to 99% of the pixels are correlated.

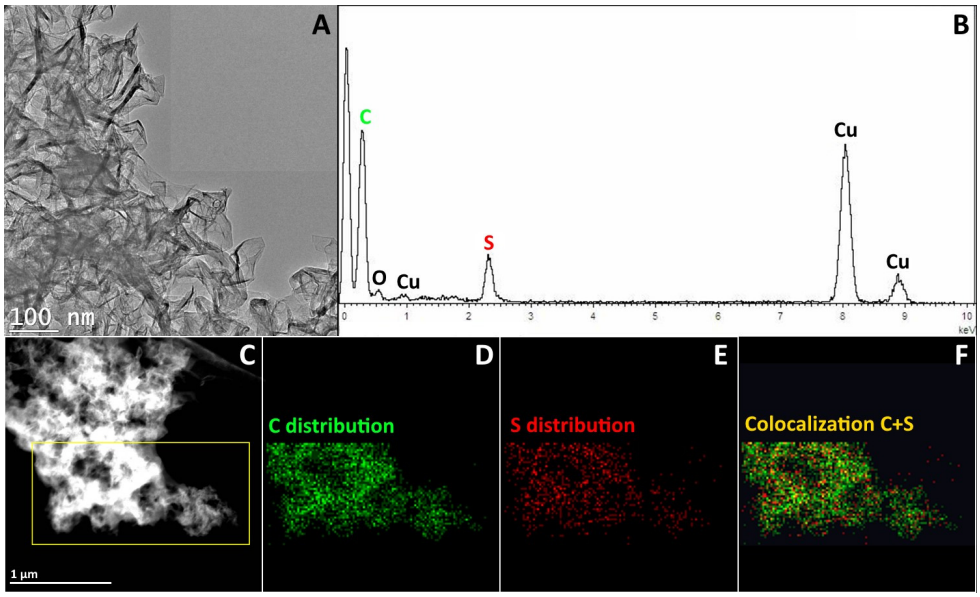

Fig. S15: **Transmission Electron Microscopy (TEM) experiments. A.** TEM image of graphene flakes after reaction with sulfur; **B.** EDX spectrum of the reacted sample. **C.** TEM image dispaying the region analysed (yellow) via EDX. **D-F** EDX images of carbon (green), sulfur (red) and their superposition , respectively, highlighting the colocalization of carbon and sulfur atoms in the reacted material.

Tables: Experimental part

Table S1: Raman peaks table of few-layer graphene before and after 24 hours of reaction.

Peak	Before reaction	After reaction	Intensity	Comments	Ref
ν(C−S)	-	**400**	Wide and weak	Similar to C−S bondings in graphdiyne sulfide	[2]
ν2: ν(S−S)	-	**495**	Narrow and weak	Possible small intercalated Sn chains	[2]
ν(C=S)	-	**1260**	Medium	Similar to thiocarbonyl	[3]
ν4: ν(C(sp^2)-SC(sp^2))	-	**1445**	Strong	Similar to observed C−S−C bondings in sulfur doped CNTs, sexithiophene and sulfur thermal reaction on a bilayer of graphene.	[4] [5] [6]
G	**1580**	**1588**	Strong	Blueshift due to p-doping and strain	[7]
ν2+ν4	-	1947	Weak	Possible association of (S−S) and v(C(sp^2)-SC(sp^2)) modes	
2D	**2690**	**2705**	Strong	Blueshift due to p-doping and strain	[7]
2*ν4	-	2890	Medium	Possible first overtone	[1]
3*ν4	-	4335	Weak	Possible second overtone	[1]

Table S2: XPS values measured on a cleaved HOPG before and after 7 days of reaction. Average values of three measurements performed on cleaved HOPG. The percentage of episulfide sulfur is extracted from the amount of S $2p_{3/2}$ C−S on the amount of S $2p_{3/2}$ C−S, C 1s sp^2 and C−S.

Attribution	Before reaction		After reaction		Ref.
	Average Peak Position (eV)	Average Atomic Percentage	Average Peak Position (eV)	Average Atomic Percentage	
C 1s C sp^2	284.4	80.5	284.4	27.93	[8]
C 1s C sp^3 C−S	-	-	285.1	38.73	[9]
C 1s C sp^2 shake up 1	291.1	6.4	290.967	3.1	[10]
C 1s C sp^2 shake up 2	294.53	0.6	-	-	[10]
C 1s C−O, epoxide	286.63	2.63	287.13	2.23	[11]
C 1s O−C=O	288.83	2.367	288.93	1.2	[11]
O 1s O−C=O·	532	2.2	-	-	[8]
O 1s C−O, epoxide, SiO_2	532.53	3.2	532.6	1.8	[8]
O 1s O·−C=O	533.567	2.1	-	-	[8]
O 1s sulfone	-	-	530.9	0.67	[8]
O 1s H_2O ads.	-	-	534.23	0.167	[8]
S $2p_{3/2}$ and $2p_{1/2}$ C=S	-	-	161.53 and 162.6	1.6	[12]
S $2p_{3/2}$ and $2p_{1/2}$ C−S	-	-	164 and 165.2	21.1	[9]
S $2p_{3/2}$ and $2p_{1/2}$ C-SO_x-C	-	-	167.3 and 168.6	0.867	[5]
Si 2p SiO_2 Quartz residue from the reaction chamber opening	-	-	103.2	0.67	[8]

Theory

Ab initio molecular dynamics

Ab initio molecular dynamics (AIMD) simulations were performed to verify the time-realized dynamical stability of the proposed GS systems. The temperature was controlled through a Nose thermostat [13] implemented in the SIESTA software package. The simulations were performed over 5 ps at a temperature of 300 K. The energy profiles are shown in Figure S16. The three systems give rise to total energy fluctuations of about twice the baseline thermal energy (∼50 meV). This is negligible both with respect to the total energy and the adsorption energies of the systems. No bond breaking or major structural changes were observed throughout the MD simulation. As such, the AIMD results support the time-resolved dynamical stability of the systems proposed herein.

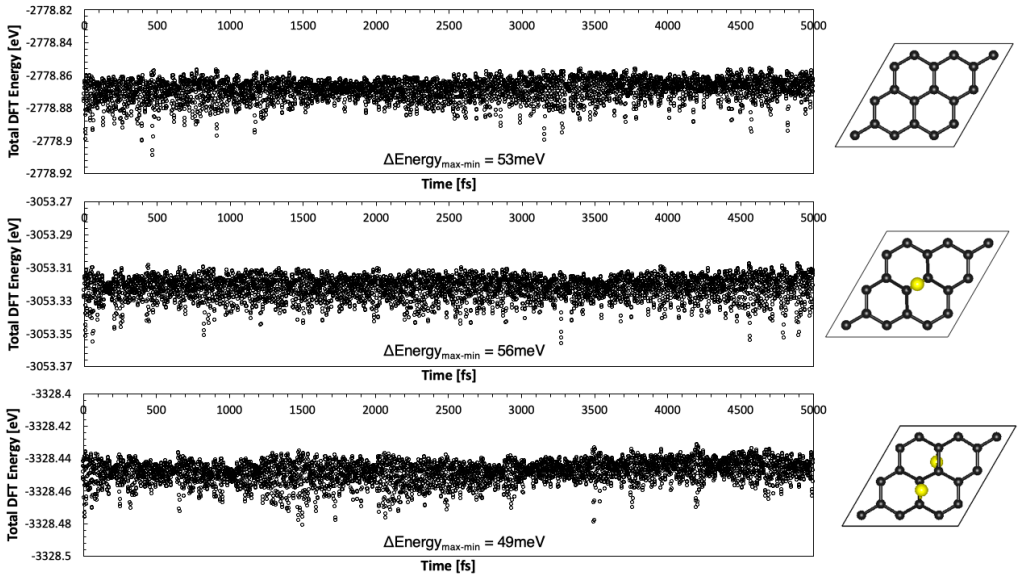

Fig. S16: **AIMD variation of total DFT calculated energy of the pristine Gr (top), GS_1 (middle) and GS_2 (bottom) systems over a 5 s timeframe with a time step of 1 fs and and a temperature of 300 K.**

Table S3: Electronic structure details for the two proposed calculated graphene-sulfur systems.

	one sulfur atom	two sulfur atoms
Sulfur coverage (%)	5.26	10.00
C−S bond length (Ang)	1.89	1.87
Orbital population overlap (Mulliken population)	0.298	0.305
S-Gr distance (Ang)	2.01	2.03
E_{ads} (eV)	2.95	3.29

Table S4: Structure details for the two proposed calculated graphene-sulfur systems.

	one sulfur atom	two sulfur atoms
a (Ang)	7.405	7.405
b (Ang)	7.405	7.405
c (Ang)	39.99	39.99
α (degrees)	90	90
β (degrees)	90	90
γ (degrees)	60	60

Vibrational Calculation Details

Γ point vibrational mode calculations were performed to verify the dynamical stability of the proposed GS systems. The interatomic force constants in real space are computed, and a discrete Fourier transform is performed to compute the dynamical matrix in reciprocal space at the Γ point. This matrix is then diagonalized, and the eigenfrequencies (and eigenvectors) are computed in order to obtain the vibrational modes. This is implemented in the VIBRA package accessible through the SIESTA software [14]. The simulations were performed on the fully relaxed pristine graphene and the proposed GS_1 and GS_2 systems using a $(3\times3\times1)$ Monkhorst-Pack mesh with the GGA-PBEsol [15] formalism and a 0.01 Å maximum displacement of the atoms. The full modes are enumerated in tables S5 through S7 for the pristine graphene, GS_1 proposed system, and the GS_2 proposed system, respectively. The three systems give rise to exactly three $\sim$0 cm^{-1} translational modes (in italic), and no major imaginary modes are observed. As such, this supports the fact that the calculations have arrived at the minimum on the potential energy surface for both systems, and the vibrational results support the dynamical stability of these systems proposed here.

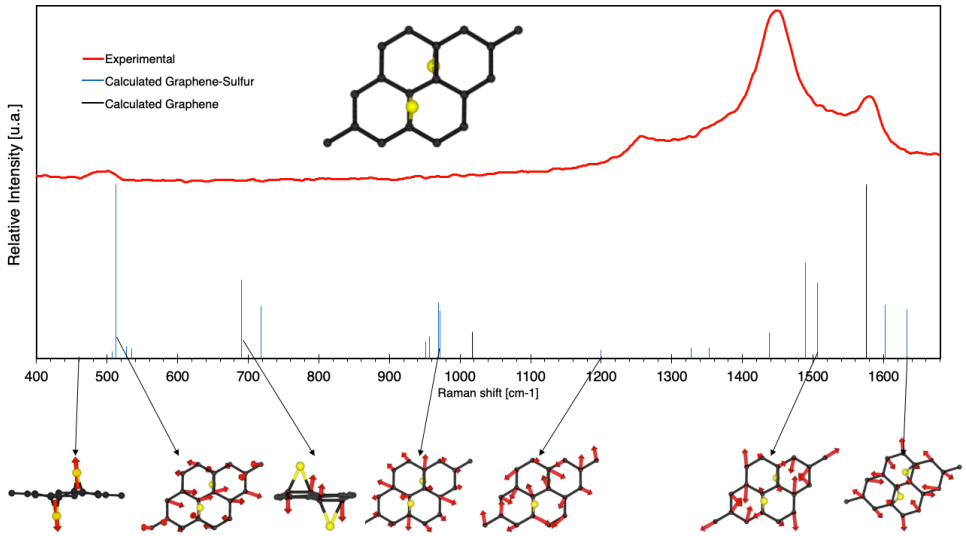

Fig. S17: **Experimental Raman spectrum of the reacted compound (top, red) and computed (bottom) first order Raman spectra of the GS_2 system (blue) and pristine (3×3) graphene (black). Intensities are normalized with respect to the maximum.**

Table S5: **List of DFT calculated Γ point vibrational modes of the graphene (no sulfur) model.**

Mode number	Mode Frequency (cm^{-1})	Mode number	Mode Frequency (cm^{-1})	Mode number	Mode Frequency (cm^{-1})
1	*-0.144014*	19	542.451147	37	1017.103041
2	*-0.057814*	20	543.099878	38	1017.533791
3	*0.010571*	21	543.103654	39	1234.734024
4	278.308961	22	758.311928	40	1234.76396
5	278.308984	23	758.312368	41	1234.814701
6	278.309187	24	758.31378	42	1234.837135
7	278.309188	25	758.31382	43	1495.166503
8	278.309637	26	758.314008	44	1495.175758
9	278.310529	27	758.314024	45	1495.305754
10	517.669859	28	861.89518	46	1495.314788
11	517.694931	29	975.610351	47	1495.594033
12	533.09092	30	975.612452	48	1495.63132
13	533.090926	31	980.050915	49	1574.593123
14	533.130899	32	980.987042	50	1574.59529
15	533.131148	33	1015.141818	51	1575.007616
16	542.359504	34	1015.566377	52	1575.315153
17	542.363238	35	1016.698496	53	1576.098425
18	542.450161	36	1017.093127	54	1576.771355

Table S6: List of DFT calculated Γ point vibrational modes of the graphene-sulfur, proposed structure GS_1).

Mode number	Mode Frequency (cm^{-1})	Mode number	Mode Frequency (cm^{-1})	Mode number	Mode Frequency (cm^{-1})
1	*-0.079407*	21	546.623404	41	1167.030179
2	*0.027662*	22	551.492028	42	1184.949922
3	*0.115832*	23	555.251154	43	1199.652207
4	137.89302	24	583.448646	44	1214.486757
5	153.289359	25	638.754705	45	1327.677895
6	179.406732	26	690.68715	46	1352.658196
7	190.547818	27	717.714806	47	1400.615914
8	254.467756	28	718.197827	48	1437.820647
9	264.053309	29	734.792725	49	1447.779684
10	278.844743	30	738.310702	50	1466.020812
11	306.594388	31	742.111195	51	1483.931772
12	338.065286	32	824.888317	52	1488.915652
13	356.811695	33	940.381731	53	1506.67037
14	435.735921	34	951.123035	54	1516.137425
15	480.82082	35	957.165052	55	1537.225417
16	507.281028	36	969.053559	56	1547.245132
17	512.769048	37	971.553419	57	1557.143826
18	520.49651	38	984.792101	58	1583.210281
19	527.238806	39	1003.677603	59	1601.883375
20	534.900251	40	1015.568611	60	1633.485776

Table S7: **List of DFT calculated Γ point vibrational modes of the graphene-sulfur, proposed structure GS_2.**

Mode number	Mode Frequency (cm^{-1})	Mode number	Mode Frequency (cm^{-1})	Mode number	Mode Frequency (cm^{-1})
1	*0.041478*	20	550.414971	39	1213.411347
2	*0.082522*	21	564.156461	40	1221.871321
3	*0.132856*	22	570.16489	41	1235.669498
4	160.853753	23	686.539553	42	1352.359322
5	175.160613	24	729.58568	43	1371.504393
6	243.976555	25	731.954573	44	1421.425416
7	261.352916	26	743.241564	45	1448.589587
8	273.622521	27	749.143546	46	1453.169944
9	276.023365	28	754.271221	47	1480.82903
10	333.334702	29	840.127291	48	1490.542976
11	343.146558	30	959.713259	49	1499.485646
12	465.153538	31	964.63426	50	1520.474935
13	504.648112	32	972.42847	51	1532.985029
14	513.729733	33	972.738762	52	1557.119077
15	519.851435	34	993.865008	53	1560.573883
16	523.948682	35	996.673314	54	1583.58242
17	528.631872	36	1014.050579	55	1605.540967
18	542.400991	37	1026.88301	56	1625.041173
19	544.537079	38	1184.134855	57	1645.57556

References

[1] Rao, R., Tishler, D., Katoch, J., Ishigami, M.: Multiphonon raman scattering in graphene. Phys. Rev. B **84**, 113406 (2011) https://doi.org/10.1103/PhysRevB.84.113406

[2] Du, H., Zhang, Z., He, J., Cui, Z., Chai, J., Ma, J., Yang, Z., Huang, C., Cui, G.: A delicately designed sulfide graphdiyne compatible cathode for high-performance lithium/magnesium–sulfur batteries. Small **13**(44), 1702277 (2017) https://doi.org/10.1002/smll.201702277 https://onlinelibrary.wiley.com/doi/pdf/10.1002/smll.201702277

[3] Lin-Vien, D., Colthup, N.B., Fateley, W.G., Grasselli, J.G.: Chapter 14 - organic sulfur compounds. In: Lin-Vien, D., Colthup, N.B., Fateley, W.G., Grasselli, J.G. (eds.) The Handbook of Infrared and Raman Characteristic Frequencies of Organic Molecules, pp. 225–250. Academic Press, San Diego (1991). https://doi.org/10.1016/B978-0-08-057116-4.50020-1 . https://www.sciencedirect.com/science/article/pii/B9780080571164500201

[4] Gaufrès, E., Tang, N.Y.-W., Favron, A., Allard, C., Lapointe, F., Jourdain, V., Tahir, S., Brosseau, C.-N., Leonelli, R., Martel, R.: Aggregation control of Î±-sexithiophene via isothermal encapsulation inside single-walled carbon nanotubes. ACS Nano **10**(11), 10220–10226 (2016) https://doi.org/10.1021/acsnano.6b05660 https://doi.org/10.1021/acsnano.6b05660. PMID: 27779852

[5] Gao, Y., Tang, Y., Liu, W., Liu, L., Zeng, X., Yan, S.: Sulfur-doped carbon nanotubes with hierarchical micro/mesopores for high performance pseudocapacitive supercapacitors. Nanotechnology **32**(50), 505401 (2021) https://doi.org/10.1088/1361-6528/ac1e52

[6] Bautista-Flores, C., Arellano-Peraza, J.S., Sato-Berrú, R.Y., Camps, E., Mendoza, D.: Sulfur and few-layer graphene interaction under thermal treatments. Chemical Physics Letters **665**, 121–126 (2016) https://doi.org/10.1016/j.cplett.2016.10.056

[7] Lee, J.E., Ahn, G., Shim, J., Lee, Y.S., Ryu, S.: Optical separation of mechanical strain from charge doping in graphene. Nature Communications **3**(1), 1024 (2012) https://doi.org/10.1038/ncomms2022

[8] Moulder, J.F.: Handbook of X-ray Photoelectron Spectroscopy: A Reference Book of Standard Spectra for Identification and Interpretation of XPS Data. Physical Electronics Division, Perkin-Elmer Corporation - 1992.

[9] Wang, F., Wang, L., Xue, Q.: Fluorine and sulfur co-doped amorphous carbon films to achieve ultra-low friction under high vacuum. Carbon **96**, 411–420 (2016) https://doi.org/10.1016/j.carbon.2015.09.084

[10] Morgan, D.J.: Comments on the xps analysis of carbon materials. C **7**(3) (2021) https://doi.org/10.3390/c7030051

[11] Al-Gaashani, R., Najjar, A., Zakaria, Y., Mansour, S., Atieh, M.A.: Xps and structural studies of high quality graphene oxide and reduced graphene oxide prepared by different chemical oxidation methods. Ceramics International **45**(11), 14439–14448 (2019) https://doi.org/10.1016/j.ceramint.2019.04.165

[12] Atzei, D., De Filippo, D., Rossi, A., Caminiti, R., Sadun, C.: Xps and laxs study of 1,3-thiazolidine-2-thione and its complexes with co(ii) and zn(ii). Spectrochimica Acta Part A: Molecular and Biomolecular Spectroscopy **51**(1), 11–20 (1995) https://doi.org/10.1016/0584-8539(94)E0083-M

[13] Nosé, S.: A unified formulation of the constant temperature molecular dynamics methods. The Journal of chemical physics **81**(1), 511–519 (1984)

[14] García, A., Papior, N., Akhtar, A., Artacho, E., Blum, V., Bosoni, E., Brandimarte, P., Brandbyge, M., Cerdá, J.I., Corsetti, F., Cuadrado, R., Dikan, V., Ferrer, J., Gale, J., García-Fernández, P., García-Suárez, V.M., García, S., Huhs, G., Illera, S., Korytár, R., Koval, P., Lebedeva, I., Lin, L., López-Tarifa, P., Mayo, S.G., Mohr, S., Ordejón, P., Postnikov, A., Pouillon, Y., Pruneda, M., Robles, R., Sánchez-Portal, D., Soler, J.M., Ullah, R., Yu, V.W.-z., Junquera, J.: Siesta: Recent developments and applications. The Journal of Chemical Physics **152**(20), 204108 (2020) https://doi.org/10.1063/5.0005077

[15] Perdew, J.P., Ruzsinszky, A., Csonka, G.I., Vydrov, O.A., Scuseria, G.E., Constantin, L.A., Zhou, X., Burke, K.: Restoring the density-gradient expansion for exchange in solids and surfaces. Physical Review Letters **100**(13), 136406 (2008) https://doi.org/10.1103/PhysRevLett.100.136406